SPINE Volume 31, Number 19, pp E682–E689

Biomechanical Comparison of Instrumented Posterior Lumbar Interbody Fusion With One or Two Cages by Finite Element Analysis

Ming-Fu Chiang, MD, PhD,* Zheng-Cheng Zhong, MS,† Chen-Sheng Chen, PhD,‡§ Cheng-Kung Cheng, PhD,‖ and Shih-Liang Shih, MD§

Study Design. Using finite element models to study the biomechanics of lumbar instrumented posterior lumbar interbody fusion (PLIF) with one or two cages.

Objective. Analyzing the biomechanics of instrumented PLIF with one or two cages as to evaluate whether a single cage is adequate for instrumented PLIF.

Summary of Background Data. Implantation of a single cage in instrumented PLIF of lumbar spine is still controversial.

Methods. Three validated finite element models of L3–L5 lumbar segment were established [intact model (INT), one cage model (LS-1), and two cages model (LS-2)]. The available finite element program ANSYS 6.0 (Swanson Analysis System Inc., Houston, TX) was applied. To analyze the biomechanics of these models, 10 Nm flexion, extension, rotation, and lateral bending moment with 150 N of preload were respectively imposed on the superior surfaces of the L3.

Results. Compared with the INT model, the decrease of ROM in the LS-1 and LS-2 models were exaggerated from 0.67° to 3.73° and ranged from 37.2% to 86.1% in all motions. The mean subsidence was found to be slightly higher in the LS-1 model. Most of the cage dislodgement in both models was less than 0.03 mm. The mean dislodgement was slightly higher in the LS-1 model. The stress of cage was found to be high in the LS-2 model. The mean stress of screw was raised to 4.5% to 9.7% in the LS-1, which was higher than that in the LS-2 model. In general, stress of adjacent disc was more pronounced in the LS-2 model. The most stress distributed at the anterior portion of the adjacent disc, which could be used to interpret the clinical findings of the early adjacent disc degeneration.

Conclusions. A single cage inserted in an instrumented PLIF gains approximate biomechanical stability, slight greater subsidence, and a slight increase in screw stress but less early degeneration in adjacent disc. Adjusting these factors, instrumented PLIF with one cage could be encouraged in clinical practice.

Key words: cage, finite element analysis, posterior lumbar interbody fusion, pedicle screw fixation, subsidence. **Spine 2006;31:E682–E689**

Since Cloward first introduced interbody fusion more than 50 years ago, posterior lumbar interbody fusion (PLIF) with pedicle screw fixation has emerged as an option for the treatment of low back pain due to spondylosis or spondylolisthesis.[1] In recent, interbody fusion with cages has been widely used. With a high fusion rate,[2–5] however, complications such as subsidence, dislodgement, or adjacent level disc degeneration may occur.[6–8]

Although the results of traditional instrumented PLIF performed with two interbody cages have been widely reported,[9] there were *in vitro* biomechanical data that demonstrated adequate stability of a single threaded interbody PLIF cage combined with a unilateral facet screw.[10] The clinical study from Molinari *et al* reported that the 2-cage group had a higher rate of dural tear and higher costs. The rates of other complications, hospital stay, fusion rates, functional outcomes, and patient satisfaction, however, did not differ between groups.[9] The recent *in vitro* study also reported that an oblique insertion of a single BAK in instrumented PLIF may reduce exposure, enable precise implantation, and significantly diminish the cost of operation.[11] To our knowledge, no study comparing the biomechanics of instrumented PLIF with a single cage or two cages using finite element analysis has been reported.

In 1974, Belytschko *et al* reported using the finite element method to study the disc-body unit of spine.[12,13] Since 1992, three-dimensional refined models have emerged.[14] The finite element model (FEM) has the advantage of easily modified cage geometry without the need for cadaver or animal specimen. Therefore, the finite element method has already been used widely for analyzing biomechanical problems and successfully in many other studies on the lumbar spine.[15–21]

To elucidate whether a single cage is adequate for instrumented PLIF, a biomechanically validated finite element model was used to analyze and compare the bio-

From the *Department of Neurosurgery, Mackay Memorial Hospital, Mackay Medicine, Nursing and Management College, Taipei Medical University, Taipei, Taiwan; †Institute of Mechanical Engineering, National Chiao-Tung University, Hsinchu, Taiwan; ‡Institute of Rehabilitation Science and Technology, National Yang Ming University, Taipei, Taiwan; §Taipei City Hospital, Taipei, Taiwan; and ‖Institute of Biomedical Engineering, National Yang Ming University, Taipei, Taiwan.

Acknowledgment date: November 15, 2005. First revision date: March 8, 2006. Acceptance date: April 17, 2006.

Supported by the Grant-MMH9238 from Department of Medical Research, Mackay Memorial Hospital, Taipei, Taiwan. This study complies with the current laws of the country in which it was performed inclusive of ethics approval.

The manuscript submitted does not contain information about medical device(s)/drug(s).

Institutional funds were received in support of this work. No benefits in any form have been or will be received from a commercial party related directly or indirectly to the subject of this manuscript.

Address correspondence and reprint requests to Chen-Sheng Chen, PhD, Institute of Rehabilitation Science and Technology, National Yang-Ming University, 155, Sec. 2, Li-Nung St., Taipei, Taiwan; E-mail: cschen@ym.edu.tw

mechanics of one or two cages in lumbar instrumented PLIF.

■ Materials and Methods

A total of three FEMs of the lumbar spine were reconstructed in this study. The first one was the intact lumbar spine. The other two fusion models were the instrumented lumbar spine implanted with a single cage or two cages.

FEM of the Intact Lumbar Spine. To create this model, computed tomography (CT) scans of L3–L5 lumbar spine of a 59-year-old healthy man were obtained. The commercially available finite element program ANSYS 6.0 (Swanson Analysis System Inc., Houston, TX) was applied to model the spinal segments. The FEM of the ligamentous lumbar spine included vertebrae, intervertebral discs, endplates, posterior elements, and the following ligaments: supraspinous, interspinous, ligamentum flavum, transverse, posterior longitudinal, anterior longitudinal, and capsular.

The material properties were assumed to be homogeneous and isotropic, and the data were adopted from the literature[21,22] (Table 1). Ligaments were simulated by the two-node link elements with resistance tension only, and elements were arranged in the anatomic direction. The cross-sectional area of each ligament was obtained from the literature[21,22] in Table 1. A 20-node solid element was used for modeling the cortical bone, cancellous bone, endplate, and disc as listed in Table 2. The disc anulus consisted of fibers embedded in the ground substance. Anulus fibers in six layers were modeled by the two-node link elements with resistance tension only and placed at an angle of 30°. The facet joint was treated as a nonlinear three-dimensional contact problem using surface-to-surface contact element, and the friction coefficient was set 0.1.[21] The initial distance between adjacent facet surfaces measured from CT findings was 1 mm. The FEM of intact lumbar spine (INT) consisted of 2,460 elements and 9,602 nodes. This INT model has acquired validation in the previous studies,[23–25] in which the stiffness of the INT model was compared with that of the cadaveric specimen in the *in vitro* test.

Table 1. Material Properties Used in FEM of the Lumbar Spine

	Young's Modulus (E:MPa)	Poisson Ratio	Cross-sectional Area (mm^2)
Material			
Cortical bone	Ex = 12000; Gxy = 4615	0.3	—
Cancellous bone	Ex = 100; Gxy = 41.7	0.2	—
Posterior elements	Ex = 3500; Gxy = 1400	0.25	—
Disc			
Nucleus	1	0.499	—
Ground substance	4.2	0.45	—
Fiber	450	0.3	0.76
Endplate	24	0.4	
Ligament			
ALL	20		63.7
PLL	20		20
TL	58.7		3.6
LF	19.5		40
ISL	11.6		40
SSL	15		30
CL	32.9		60
Spinal instrumentation (titanium alloy)	110,000	0.28	
Spinal cage (titanium alloy)	110,000	0.28	

ALL = anterior longitudinal ligament; PLL = posterior longitudinal ligament; TL = transverse ligament; LF = ligamentum flavum; ISL = interspinous ligament; SSL = supraspinous ligament; CL = capsular ligament.

Table 2. Element Type Used in the FEM of the Lumbar Spine

Spine	Element Type
Vertebrae	
Cortical bone	20-node solid 95
Cancellous bone	20-node solid 95
Posterior element	20-node solid 95
Disc	
Ground substance	20-node solid 95
Nucleus	20-node solid 95
Endplate	20-node solid 95
Fiber	2-node link10
Spinal cage	
Cage	20-node solid 95
Contact surface	8-node contact 174
Target surface	Target 170
Facet joint	
Contact surface	8-node contact 174
Target surface	Target 170
Ligament	
ALL	2-node link10
PLL	2-node link10
TL	2-node link10
LF	2-node link10
ISL	2-node link10
SSL	2-node link10
CL	2-node link10
Spinal instrumentation	
Rod and screw	2-node beam 188

FEM of PLIF With Instrumentation. To simulate the PLIF, total laminectomy, medial facetectomy, and discectomy were performed on the L4–L5 motion segment. The posterior elements, supraspinous, interspinous, ligamentum flavum ligaments, medial part of the facet joint, and the partial disc were removed and implanted by the spinal cage and instrumentation system.

Instrumented PLIF With Cage Model. The intact FEM model described above was modified to simulate the instrumented PLIF with one cage (LS-1) or two cages (LS-2). In this model, four pedicle screws (r = 6 mm) simulated were inserted through the pedicles and connected by two rods (r = 6 mm) modeled with three-dimensional beam elements. Two RF (A-Spine Inc.) cages (titanium, 12 mm × 16 mm × 24 mm) (Figure 1) were placed between the vertebral bodies within the

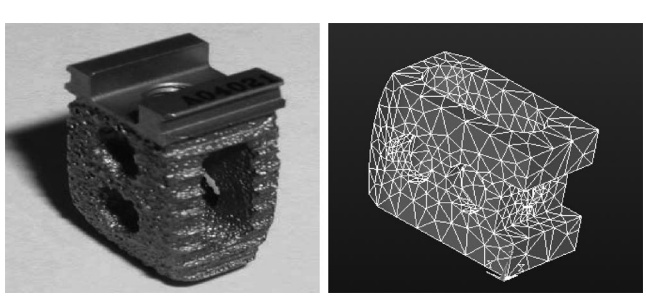

Figure 1. RF cage (left), FEM model (right).

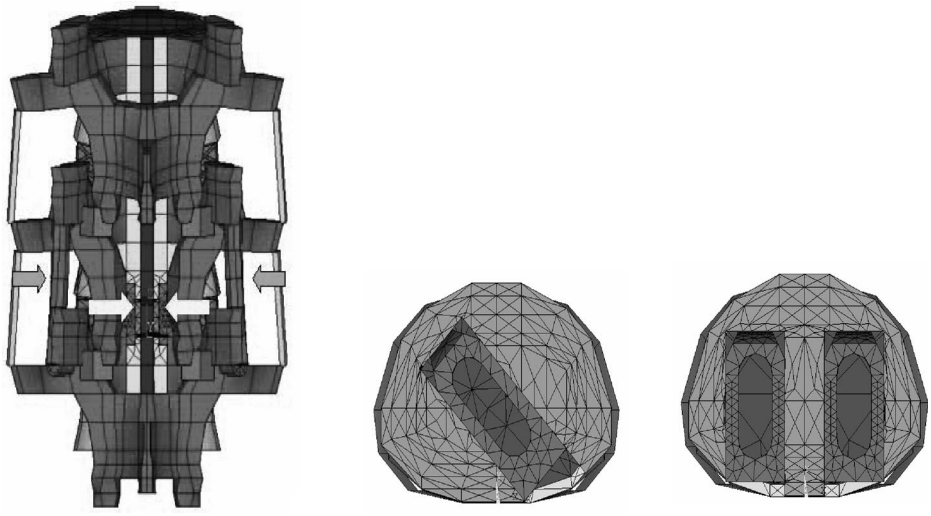

Figure 2. FEM of instrumented PLIF with one cage (LS-1 model) (**A**) or with two cages (LS-2 model) (**B**).

posterior two thirds of the disc space on the transverse plane, and covered a contact area of 239 mm^2. Single RF (A-Spine Inc.) cage (titanium, 12 mm × 16 mm × 30 mm) was obliquely inserted by 45°, and covered contact area of 191.5 mm^2. The bone-cage interface was modeled by surface-to-surface contact elements to simulate early postoperative stage after implantation of spinal cage. These contact elements are able to transmit compression forces but not tension. Most cages have small teeth on the contact surfaces that are supposed to prevent movement of the cage, so a higher friction coefficient of 0.8 was defined between the cage and the adjacent vertebrae.[21] For fusion model, two types of models were built, by changing the parameters for examination of the effects of a single cage (Figure 2A) and two cages (Figure 2B). This FEM of the lumbar spine with two RF cages consisted of 16,808 elements and 26,529 nodes.

Boundary and Loading Condition. In these models, the inferior surfaces of the L5 vertebral body were fixed completely. The lumbar spine was subjected to the maximal possible load without causing spinal injury, so the 10 N-m flexion, extension, rotation, and lateral bending moment with the 150 N of the preload were respectively imposed on the superior surfaces of the L3 vertebral body.[26]

Validation of the Model. To validate the model, the same loading condition as given in the Yamamoto *et al* study was applied.[26] Therefore, the 10 Nm flexion, 10 Nm extension, 10 Nm rotation, and 10 Nm lateral bending movement under 150 N preloads were imposed on the L3 vertebral body, respectively. Because of the stress accumulation caused by different loads, it was necessary to consider the overall stress variation in the estimated results of the FEM. Consequently, the stress results were expressed in term of von Mises stresses. The estimation of stress increase rate of the adjacent disc is shown in the following equation: Stress increase rate = (S/fused − S/intact)/(S/intact) (%), where S/fused and S/intact represent the maximum von Mises stress of the adjacent disc in the fused model and the intact model, respectively. The cage subsidence is computed on axial deformation of vertebral body contacting to spinal cage.

■ Results

Model Validation

To validate our model, the computed gross response characteristics with available experimental results was compared. Our results of the FEM under the act of the same load was compared with the kinematic data of the lumbar spine reported previously.[1,24,26] We found a good agreement between our results and the reported data (Tables 3, 4).[1,26] In addition, the intact results served as baseline data for our interpretation of the results of the fusion models.

Kinematics Analysis of the 3 FEMs

The biomechanical behavior of the instrumented PLIF with one or two cages were respectively compared with that of the intact lumbar spine.

Range of Motion (ROM)

The ROM of LS-1 and LS-2 were high in rotation with a mean of 1.27° (range, 1.06°–1.41°). In other loading motions, the ROM was less than 1° (Table 3). When compared with the INT model, the decrease of ROM in the LS-1 and the LS-2 model was exaggerated from 0.67

Table 3. Comparison of ROM in Degree of 3 Models and the *In Vitro* Study in Different Loading Motions[26]

Model	Flexion (°)	Extension (°)	Right Rotation (°)	Left Rotation (°)	Right Bending (°)	Left Bending (°)
Yamamoto *et al*	7.1	4.0	2.4	1.4	3.8	3.8
INT	4.49	3.89	2.08	2.08	3.75	3.75
LS-1	0.78	0.54	1.29	1.41	0.79	0.76
LS-2	0.76	0.64	1.31	1.06	0.71	0.70

Table 4. Comparison of ROM Decrease Between the FEM and the *In Vitro* Study[1]

	Flexion (%)	Extension (%)	Rotation (%)	Lateral Bending (%)
LS-1	82.6	86.1	37.2	79.2
LS-2	83.1	83.6	43.3	81.4
Morlock *et al*	86	89	34	75

(2.08 − 1.41 = 0.67) in left rotation of LS-1 to 3.73 (4.49 − 0.76 = 3.73) degrees in flexion of LS-2 (Table 3). The decrease of ROM in all motions ranged from 37.2% to 86.1% (Table 4). In lateral bending, the ROM of the LS-1 and LS-2 fusion models were respectively reduced to 79.2% and 81.4% compared with the INT model. In flexion, these two fusion models almost had the same ROM (Table 3). The difference of decrease in range of motion in both groups was within 5% (Table 4). Compared with a previous study, the trend of FEM calculation was similar to the trend of the Morlock *et al*[1] *in vitro* test in flexion, extension, and lateral bending as listed in Table 4.

Maximum Subsidence and Dislodgement

Subsidence of these two fusion models was relatively small as listed in Table 5. The greatest subsidence was found in flexion, which was 0.15 mm in the LS-1 and 0.09 mm in the LS-2 model, respectively. The mean subsidence was found to be slightly higher in LS-1 model (Figure 3). Most of the maximum dislodgement of cage in both models were less than 0.03 mm. In rotation motion, the dislodgement of cage in the LS-1 model was 0.25 mm, which was greater than that of the LS-2 model (0.18 mm) (Table 5). The mean dislodgement was slightly higher in LS-1 model (Figure 4).

Table 5. Comparison of the Maximum Subsidence and Dislodgement of Cage

Maximum Subsidence/ Maximum Dislodgement	Model LS-1	Model LS-2
Flexion		
Maximum subsidence (mm)	0.15	0.09
Maximum dislodgement (mm)	0.03	0.03
Extension		
Maximum subsidence (mm)	0.01	0.01
Maximum dislodgement (mm)	0.02	0.01
Right rotation		
Maximum subsidence (mm)	0.05	0.04
Maximum dislodgement (mm)	0.13	0.17
Left rotation		
Maximum subsidence (mm)	0.06	0.04
Maximum dislodgement (mm)	0.25	0.18
Right bending		
Maximum subsidence (mm)	0.06	0.05
Maximum dislodgement (mm)	0.02	0.02
Left bending		
Maximum subsidence (mm)	0.07	0.05
Maximum dislodgement (mm)	0.01	0.02

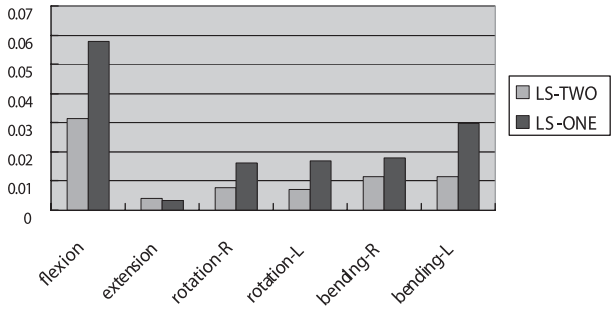

Figure 3. The mean subsidence (mm) of cage in LS-1/LS-2 model.

Stress of Cage

The stress of cage was found to be high in LS-2 model (Figure 5). In right lateral bending, the maximum stress of the cage reached 44.9 MPa in LS-2 model and 36.4 MPa in LS-1 model. The largest difference of stress in both models was found in extension, where 0.04 MPa occurred in the LS-1 and 0.27 MPa in the LS-2 model (Table 6). In flexion, the difference of stress between both models was least, and most stress was distributed at the posterior part of cage (Figure 6).

Stress of Pedicle Screw

The largest stress of pedicle screw was found with 105 MPa in the LS-1 model under right rotation loading. The smallest stress of pedicle screw was 61 MPa in the LS-2 model under extension loading (Table 6). The mean stress of screw was raised to 4.5% to 9.7% in the LS-1, which was higher than that in the LS-2 model (Figure 7).

Stress of the Adjacent Disc (L3–L4 Disc)

The maximum stress of the adjacent disc superior to the fused level occurred in the LS-1 model with the magnitude of 1.22 MPa under right bending, and in the LS-2 model with 1.46 MPa under rotation loading. In flexion and extension, the disc stress of the two fusion models apparently increased when compared with the INT model (Table 6). In general, stress of adjacent disc was more pronounced in the LS-2 model (Figure 8). The most stress distributed at the anterior portion of the adjacent disc, which could be used to interpret the clinical findings of the early adjacent disc degeneration (Figure 9).

■ Discussion

The results of traditional PLIF with 2 structural interbody cages have been widely reported.[9] Zhao *et al* re-

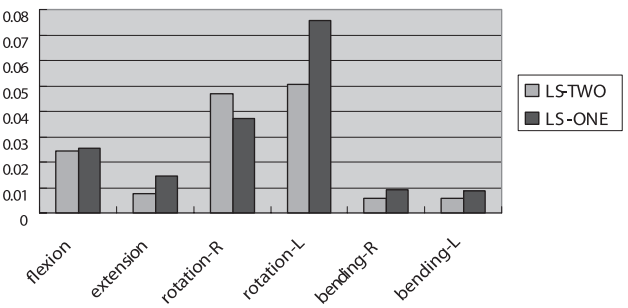

Figure 4. The mean dislodgement (mm) of cage in LS-1/LS-2 model.

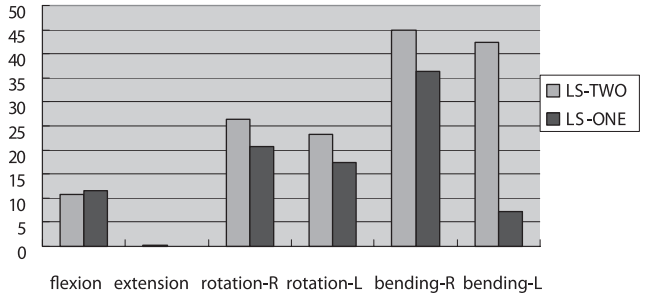

Figure 5. Stress (MPa) of cage in LS-1/LS-2 model.

cently published bovine biomechanical data demonstrating adequate stability of a single threaded interbody PLIF cage when combined with a unilateral facet screw.[10] Critics of the bilateral PLIF procedure included the increased risk of complications with excessive epidural bleeding and prolonged or excessive dural retraction. Elias *et al* reported a 15% incidence of dural tear and postoperative radiculopathy in 67 patients who had PLIF using bilateral cages.[27] Okuyama *et al* reported an 8% incidence of neurologic impairment after instrumented PLIF procedures and concluded that the bilateral procedure is technically demanding, with a high overall complication rate.[28] Molinari *et al* reported the difference in costs between 1 cage and 2 cages was $1,728.[9] In addition to cost savings, there are theoretical advantages of performing instrumented PLIF using only a single interbody cage through a unilateral approach.[9]

We used for the first time the FEM to analyze the biomechanics of one or two cages in lumbar instrumented PLIF. The model allows us to repeat experiments, to change parameters, thus analyzing the effect and influence of a single component within the construct investigated.[20,23] The procedure of merging the CAT and FEM does not require manual digitization of the images. The realistic three-dimensional geometry, accurate modeling of nonhomogeneous composite structure of intervertebral discs, and consideration of large contact phenomenon at facet joints and of the compliance of bony vertebrae by deformable beam elements make the current model one of the most detailed developed research methods.[29–31]

Table 6. Stress of Cage, Pedicle Screw, and Adjacent Disc

	Model	
Stress	LS-1	LS-2
Flexion		
Cage stress (MPa)	11.5	10.7
Screw stress (MPa)	72.4	73.4
Disc stress (MPa)	1.02	1.00
Extension		
Cage stress (MPa)	0.04	0.27
Screw stress (MPa)	66.9	61
Disc stress (MPa)	0.77	1.09
Right rotation		
Cage stress (MPa)	20.8	26.3
Screw stress (MPa)	105	96.1
Disc stress (MPa)	0.97	1.46
Left rotation		
Cage stress (MPa)	17.3	23.3
Screw stress (MPa)	97	97.2
Disc stress (MPa)	0.97	1.46
Right bending		
Cage stress (MPa)	36.4	44.9
Screw stress (MPa)	83.5	77.3
Disc stress (MPa)	1.2	1.27
Left bending		
Cage stress (MPa)	7.15	42.3
Screw stress (MPa)	81.4	77.9
Disc stress (MPa)	1.22	1.22

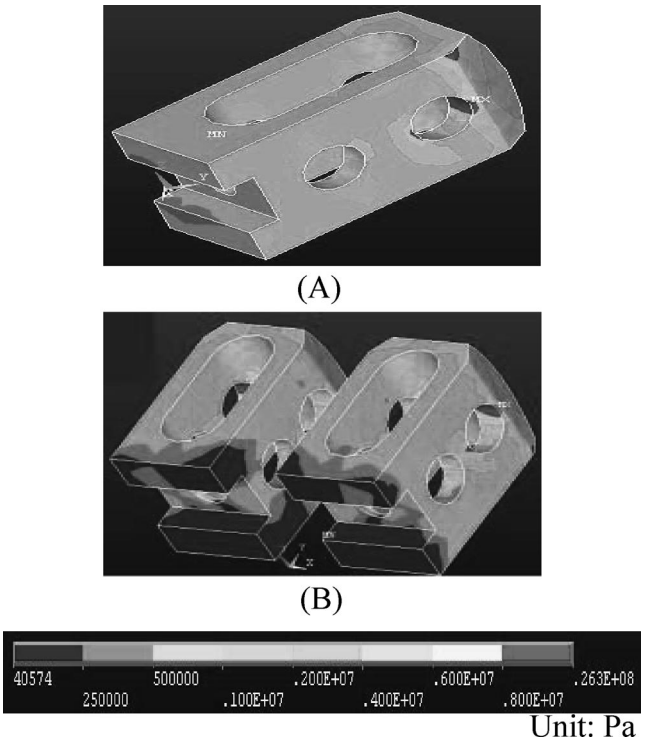

Figure 6. In flexion loading, comparing the stress of cages in two models. The most stress distributed at the posterior part of cage: (**A**) one cage, (**B**) two cages.

Model Validation

The FEM model should be interpreted as a trend only. The material properties are not exactly known for human tissues. Because of the variability of different human tissues, the FEM does not necessarily reflect the behavior of all specimens tested in the experimental part of the

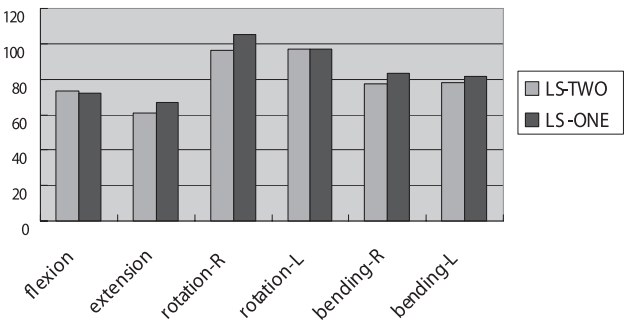

Figure 7. Screw stress (MPa) in LS-1/LS-2 model.

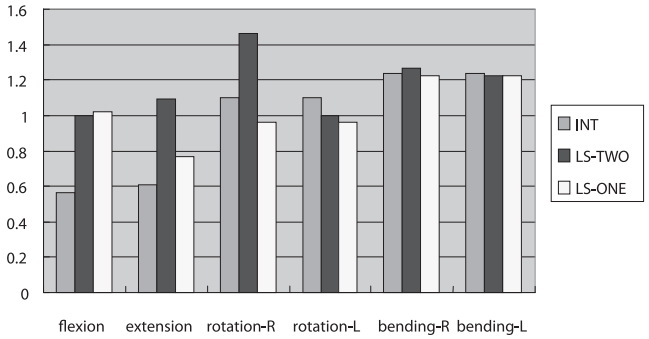

Figure 8. Adjacent disc stress (MPa) in INT/LS-1/LS-2 model.

study. Thus, major differences when compared with results of *in vitro* studies may occur, as have been observed in the current study.[1,11,26] The validation of finite element models is generally effected through a comparison between the results yielded by the models and the experimental studies.[14,20] Based on the results of the validation process as described, this FEM has been validated sufficiently.[1,26]

ROM

The difference of decrease in range of motion in both LS-1 and LS-2 models was within 5%. This disclosed that these two fusion models were able to achieve the approximate stability. The ROMs of both models were high in rotation with a mean of 1.27°. It was lower when compared with the data from Yamamoto *et al* (mean = 1.9)[26] (Table 3). The reason may be due to one side or bilateral medial facetectomies made the curvature of facet joint of this FEM different to that of cadaveric specimen, and linear simulation of facet capsule in FEM was different with actual facet capsule.[23–25]

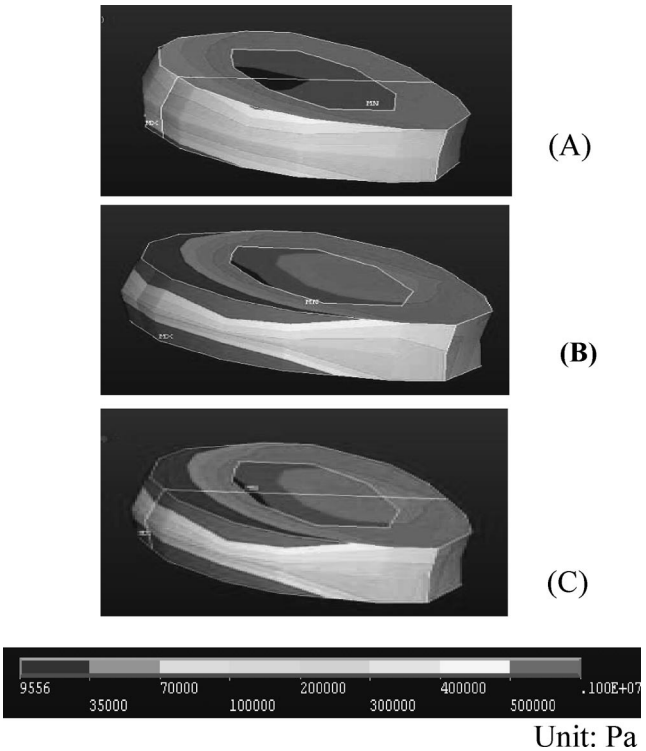

Figure 9. In flexion loading, comparing the stress of adjacent disc in three models: (**A**) INT model; (**B**) LS-1 model; (**C**) LS-2 model. The most stress distributed at the anterior portion of the adjacent disc.

Subsidence and Dislodgement

Subsidence is a complication of cage sinking with loss of normal intervertebral height. Eck *et al* indicated that 14% of patients had this complication after a 2-year follow-up.[6] Subsidence of these two fusion models was relatively small. The mean subsidence was greater in the LS-1 model. Because the LS-1 model has less contact area than the LS-2 model, the contact pressure in the LS-1 model was more intensively distributed onto vertebral body and thus caused greater subsidence. The greatest subsidence was found in flexion loading of LS-1 model. This indicated that cage subsidence was prone to occur in LS-1 model under flexion loading.

The complication of cage dislodgement occurred in approximately 1.4% of patients.[27] Except for the rotation motion, the dislodgement of cage in both models was less than 0.03 mm. In rotation motion, the dislodgement of the LS-1 model was also greater than that of the LS-2 model. The mean dislodgement was slight large in LS-1 model. Kim reported that the maximum dislodgement would occur in rotation with a preload, which was consistent with our FEM calculation.[16]

Stress of Cage and Pedicle Screw

The stress of cage was found to be high in the LS-2 model. Most stress of cage in both models was distributed at the posterior part of cage. In flexion, the difference of stress between the LS-1 and LS-2 models was least. From a mechanical point of view, the stability of the cage was increased following with more contact stress between cage and vertebral body. The stress of pedicle screw was found to be largest in rotation loading of the LS-1 model. The smallest stress of pedicle screw occurred in extension of the LS-2 model. The mean stress of screw was raised to 4.5% to 9.7% in the LS-1 than that in the LS-2 model. The LS-1 model shifted more stress to the screw, which could elucidate why the breakage of screw may occur often in this model.

Stress of the Adjacent Disc

The early degeneration of adjacent disc had been reported by Kuslich *et al* to be 5.6% in his patients.[7] Lehmann *et al* reported accelerated degeneration of adjacent segment and segmental instability above the fusion occurred 5% of their patients.[32] Frymoyer *et al* reported that symptomatic adjacent disc disease occurred in 5 of their 143 fusion patients.[33] The biomechanical studies with FEM addressed that the stress of the adjacent disc increased within 20% compared with the disc of the intact spine.[4,8,17,25] In our FEM study, the disc stress of both fusion models apparently increased in flexion and extension, when compared with the INT model. The greatest raise reached to 80.95% in the LS-1 model under flexion loading. Most of the stress distributed at the

anterior portion of adjacent disc, which could interpret the clinical findings of early degeneration of adjacent disc.[33–35] Consequently, the stress of adjacent disc is possibly to increase more since the bone graft completely fused to vertebral body would give rise to greater stiffness of motion segment. As a result, the adjacent disc was likely to accelerate degeneration under situation of stress concentration.

Study Limitation

Regarding the limitation and restriction of this study, the material property of this FEM was different with that of cadaver specimen, such as nonlinear behavior of spinal ligaments, viscoelasticity of disc, and orthotropic characteristics of vertebral body.[23–25,36,37] The loading conditions we used may not so clinically relevant as that of Goel hybrid approach.[38] A physiologic condition should be involved in the application of overall displacement for fusion model equal to the intact model by varying different moments.[38] The FEM did not account for the mechanical effect of muscle contraction.[39] The effect of these FEM simulations was similar to that of the *in vitro* test, so the muscle contraction, complicated external load, the movement of pelvis, and completeness of entire spine were not considered in this study. Clinically, when spinal cages are implanted, the disc space is distracted, leading to tension in the anular fibers. It is thought that the contracting fibers produce compression between the cage and the vertebrae, maintaining the cage in place.[40] In our study, this mechanism was not modeled.

Based on the results of this study, a single cage inserted in an instrumented PLIF gains, excepting the cost benefit and the operative feasibility, the approximate biomechanical stability, the slight greater subsidence, and a slight increase in screw stress but less early degeneration in adjacent disc. Adjusting these factors, instrumented PLIF with one cage could be encouraged in clinical practice. The present investigation reinforces the concept that a realistic model study, concurrent with experimental and clinical validations, is an appropriate approach toward the elucidation of the complex biomechanical dynamics of the human lumbar spine.

■ Conclusion

A three-dimensional nonlinear finite element model of the lumbar spine was established to simulate the instrumented PLIF with cage. A single cage inserted in instrumented PLIF caused an approximate stability and resulted in less stress in adjacent disc than that of the LS-2 model. We therefore recommended that a single cage is adequate in an instrumented PLIF. Considerable progress in research appears to be needed for the achievement of a satisfactory understanding of the biomechanics of the instrumented PLIF with cage in human lumbar spine.

■ Key Points

- A three-dimensional nonlinear FEM of the lumbar spine was established to simulate the instrumented PLIF with cages.
- A single cage inserted in instrumented PLIF caused an approximate stability and resulted in less stress in adjacent disc than that of the LS-2 model.
- Implantation of a single cage in an instrumented PLIF is adequate.

References

1. Morlock MM, Strandborg J, Nassutt R, et al. Primary stability of dorsal lumbar spondylodesis and vertebral body replacement surgery: comparison of different vertebral body replacement cages in-vitro. *47th Annual Meeting of the Orthopaedics Research Society*, San Francisco, 2001.
2. Brantigan JW, McAfee PC, Cunningham BW, et al. Interbody lumbar fusion using a carbon fiber cage implant versus allograft bone: an investigational study in the Spanish goat. *Spine* 1994;19:1436–44.
3. Brantigan JW, Steffee AD. A carbon fiber implant to aid interbody lumbar fusion: two-year clinical results in the first 26 patients. *Spine* 1993;18:2106–17.
4. Matge G. Cervical cages fusion with 5 different implants: 250 cases. *Acta Neurochir* 2002;144:539–49.
5. Ray CD. Threaded titanium cages for lumbar interbody fusions. *Spine* 1997;22:667–79.
6. Eck KR, Bridwell KH, Ungacta FF, et al. Analysis of titanium mesh cages in adults with minimum two-year follow-up. *Spine* 2000;25:2407–15.
7. Kuslich SD, Danielson G, Dowdle JD, et al. Four-year follow-up results of lumbar spine arthrodesis using the Bagby and Kuslich lumbar fusion cages. *Spine* 2000;25:2656–62.
8. McAfee PC. Interbody fusion cages in reconstructive operations on the spine. *J Bone Joint Surg Am* 1999;81:859–80.
9. Molinari RW, Sloboda J, Johnstone FL. Are 2 cages needed with instrumented PLIF? A comparison of 1 versus 2 interbody cages in a military population. *Am J Orthop* 2003;32:337–43.
10. Zhao J, Hai Y, Ordway NR, et al. Posterior lumbar interbody fusion using posterolateral placement of a single cylindrical threaded cage. *Spine* 2000;25:425–30.
11. Wang ST, Goel VK, Fu CY, et al. Posterior instrumentation reduces differences in spine stability as a result of different cage orientations: an *in vitro* study. *Spine* 2005;30:62–7.
12. Belytschko T, Kulak RF, Shultz AB. Finite element stress analysis of an intervertebral disc. *J Biomech* 1974;7:277–85.
13. Totoribe K, Tajima N, Chosa E. A biomechanical study of posterolateral lumbar fusion using a three-dimensional nonlinear finite element method. *J Orthop Sci* 1999;4:115–26.
14. Lavaste F, Skalli W, Robin S, et al. Three-dimensional geometrical and mechanical modeling of the lumbar spine. *J Biomech* 1992;25:1153–64.
15. Adam C, Pearcy M, McCombe P. Stress analysis of interbody fusion: finite element modeling of intervertebral implant and vertebral body. *Clin Biomech* 2003;18:265–72.
16. Kim Y. Prediction of mechanical behaviors at interfaces between bone and two interbody cages of lumbar spine segments. *Spine* 2001;26:1437–42.
17. Palm WJ, Rosenberg WS, Keaveny TM. Load transfer mechanisms in cylindrical interbody cages constructs. *Spine* 2002;27:2101–7.
18. Pitzen T, Geisler FH, Matthis D, et al. The influence of cancellous bone density on load shearing in human lumbar spine: a compression between an intact and surgically altered motion segment. *Eur Spine J* 2001;10:23–9.
19. Pitzen T, Geisler FH, Matthis D, et al. Motion of threaded cages in posterior lumbar interbody fusion. *Eur Spine J* 2000;9:571–6.
20. Pitzen T, Matthis D, Steudel WI. The effect of posterior instrumentation following PLIF with BAK cages is most pronounced in weak bone. *Acta Neurochir* 2002;144:121–8.
21. Polikeit A, Ferguson SJ, Nolte LP, et al. Factors influencing stresses in the lumbar spine after the insertion of intervertebral cages: finite element analysis. *Eur Spine J* 2002;12:413–20.
22. Goel VK, Monroe BT, Gilbertson LG, et al. Interlaminar shear stresses and laminae separation in a disc: finite element analysis of the L3–L4 motion segment subjected to axial compressive loads. *Spine* 1995;20:689–98.

23. Chen CS, Cheng CK, Liu CL, et al. Stress analysis of the disc adjacent to interbody fusion in lumbar spine. *Med Eng Phys* 2001;23:483–91.
24. Chen CS, Cheng CK, Liu CL. A biomechanical comparison of posterolateral fusion and posterior fusion in the lumbar spine. *J Spinal Disorder Tech* 2002;15:53–63.
25. Chen CS, Feng CK, Cheng CK, et al. Biomechanical analysis of the disc adjacent to posterolateral fusion with laminectomy in lumbar spine. *J Spinal Disorder Tech* 2005;18:58–65.
26. Yamamoto I, Panjabi MM, Crisco T, et al. Three-dimensional movement of the whole spine and lumbosacral joint. *Spine* 1989;14:1256–60.
27. Elias WJ, Simmons NE, Kaptain GJ, et al. Complications of posterior lumbar interbody fusion using a titanium threaded cage. *J Neurosurg* 2000; 93:338–40.
28. Okuyama K, Suzuki T, Tamura Y, et al. Posterior interbody fusion: a retrospective study of complications after facet joint excision and pedicle screw fixation in 148 cases. *Acta Orthop Scand* 1999;70:329–34.
29. Shirazi-Adl A, Parnianpour M. Nonlinear response analysis of the human ligamentous lumbar spine in compression: on mechanisms affecting the postural stability. *Spine* 1993;18:147–58.
30. Shirazi-Adl A. Nonlinear stress analysis of the whole lumbar spine in rotation-mechanics of facet articulation. *J Biomech* 1994;27:289–99.
31. Shirazi-Adl A. Biomechanics of the lumbar spine in sagittal/ lateral moments. *Spine* 1994;19:2407–14.
32. Lehmann TR, Tozz JE, Weinstein JN, et al. Long term follow up of lower lumbar fusion patient. *Spine* 1987;12:97–103.
33. Frymoyer JW, Hanley E, Howe J, et al. Disc excision and spine fusion in the management of lumbar disc disease. *Spine* 1978;3:1–6.
34. Takahashi K, Kitahara H, Yamagata M, et al. Long-term results of anterior interbody fusion for treatment of degenerative spondylolisthesis. *Spine* 1990;15:1211–5.
35. Schlegel JD, Smith JA, Schleusener RL. Lumbar motion segment pathology adjacent to thoracolumbar, lumbar, and lumbosacral fusions. *Spine* 1996; 21:970–81.
36. Lee CK, Kim YE, Lee CS, et al. Impact response of the intervertebral disc in a finite-element model. *Spine* 2000;25:2431–9.
37. Qiu TX, Teo EC, Lee KK, et al. Validation of T10–T11 finite element model and determination of instantaneous axes of rotations in three anatomical planes. *Spine* 2003;28:2694–9.
38. Goel VK, Grauer JN, Patel TC, et al. Effects of Charite artificial disc on the implanted and adjacent spinal segments mechanics using a hybrid testing protocol. *Spine* 2005;30:2755–64.
39. Goel VK, Kong WZ, Han JS, et al. A combined finite element and optimization investigation of lumbar spine mechanics with and without muscles. *Spine* 1993;18:1531–41.
40. Bagby GW. Arthrodesis by the distraction-compression method using a stainless steel implant. *Orthopedics* 1988;11:931–4.